Desalination and Water Treatment
www.deswater.com

doi:10.5004/dwt.2017.20527

77 (2017) 306–314
May

Inhibition of calcium carbonate and sulfate scales by a polyether-based polycarboxylate antiscalant for cooling water systems

Ao Zhang[a,b], Yuming Zhou[a,b,*], Qingzhao Yao[b,*], Tiantian Wang[b], Jun Li[b], Yiyi Chen[b], Qiuli Nan[a], Mingjue Zhang[a], Wei Sun[c], Wendao Wu[c]

[a]*Cheng Xian College, Southeast University, Nanjing 210008, China, Tel. +86 13770899929; email: 53212651@qq.com (Q. Nan), Tel. +86 13805195819; email: 489354839@qq.com (M. Zhang)*
[b]*School of Chemistry and Chemical Engineering, Southeast University, Nanjing 211189, China, Tel. +86 25 52090617; emails: ymzhou@seu.edu.cn (Y. Zhou); 101006377@seu.edu.cn (Q. Yao), 220142382@seu.edu.cn (A. Zhang), 1439127031@qq.com (T. Wang), 1543107327@qq.com (J. Li), 838331357@qq.com (Y. Chen)*
[c]*Jianghai Environmental Protection Co., Ltd, Changzhou 213116, China, Tel. +86 25 52090617; emails: leojhhg@sina.com (W. Sun), 13887303@qq.com (W. Wu)*

Received 25 September 2016; Accepted 17 January 2017

ABSTRACT

To inhibit calcium carbonate and sulfate scales in cooling water systems, a new antiscalant (acrylic acid–oxalic acid–methallyl methoxy polyethylene glycol, [AA-HPEZ]) was synthesized via radical copolymerization, and the structure of inhibitors was characterized by Fourier Transform infrared spectroscopy, hydrogen Nuclear magnetic resonance, and carbon thirteen Nuclear magnetic resonance. The ability of the polymer to mitigate the calcium carbonate and calcium sulfate scales formation was tested by static scale inhibition methods. The inhibition efficiencies of AA-HPEZ toward $CaCO_3$ and $CaSO_4$ scales were 90.6% and 100%, with 8 and 4 mg/L, respectively. The performance of copolymer on inhibition to $CaCO_3$ and $CaSO_4$ precipitation was better than poly(acrylic acid), poly(epoxysuccinic acid), and hydrolytic poly(maleic anhydride). AA-HPEZ shows great antiscaling properties for $CaCO_3$ scale even for the solution with higher temperature and higher hardness.

Keywords: Crystallization; Scale inhibition; Copolymer; Calcium carbonate; Calcium sulfate

1. Introduction

The deposition of calcium containing scales such as calcium carbonate, calcium sulfate, and calcium phosphate has become a significant problem in large commercial water treatment processes with the wide application of circulating cooling water systems [1–3]. The formation of scales mainly depends on pH, temperature, pressure, and minerals concentration of the cooling water [4]. The formation of scales causes great problems from both economic and technical point of view, such as reduced efficiency of heat transfer and increased frictional resistance between the water and equipment surfaces [5–8].

Currently, there are three main routes to mitigate the problem of scaling: (1) use of water softening chemicals, (2) mechanical cleaning, and (3) using chemical treatment methods [9,10]. The use of scale inhibitors is the most effective and economical method which can achieve the purpose of decreasing the rate of scale growth by absorbing at the active growth sites on the crystal surface [11]. Polyphosphate types inhibitors are most widely used to prevent minerals deposition on pipes and heat exchanger surfaces in cooling systems [12,13]. However, polyphosphate inhibitors are likely to decompose and form orthophosphate which can react with calcium ions to form relatively insoluble calcium phosphate scale due to the increase in temperature [14]. In addition, they also cause secondary pollution and ecological imbalance

* Corresponding author.

in water [15]. The deposition of calcium is mainly constituted of calcium carbonate and calcium sulfate [16,17]. Thus, environmentally friendly green scale inhibitors have caught more attention in recent years due to the major concern over global ecological and environmental problems [18]. Polycarboxylate is another widely used class of the scale inhibitors which usually contains a cyclic or linear structure [19]. Unfortunately, most of polycarboxylate scale inhibitors show a low calcium tolerance and can react with calcium ions to form insoluble calcium–polymer salts [20]. Poly(aspartic acid) and anhydride containing alternating copolymers have been evaluated for its efficiency on scales inhibition in cooling water systems due to their good biodegradability and chelating ability [17,21]. However, they all show poor inhibition in a high-temperature environment which markedly limits its wide use [22]. As a result, an ideal antiscalant should be effective to prevent and inhibit the deposition of calcium carbonate and calcium sulfate at high temperature.

Compared with allyloxy polyethoxy ether (APEG), methallyl methoxy polyethylene glycol (HPEG) has a broader choice of comonomer to synthesize copolymer as a scale inhibitor [23]. In recent years, our group has prepared various scale inhibitors based on APEG to control the depositions of calcium carbonate and calcium sulfate [24–28]. However, there have been no reports about polymer based on HPEG used as a scale inhibitor for cooling water systems.

In this study, we prepared new effective non-phosphorus scale inhibitors (acrylic acid–oxalic acid–methallyl methoxy polyethylene glycol [AA-HPEZ]) to control the calcium carbonate and calcium sulfate depositions in cooling water systems. The new inhibitor is a kind of double-hydrophilic block copolymer whose structure contains many functional groups such as carboxyl, allyloxy, and ester. These functional groups provide AA-HPEZ with a number of advantages, for example, simple experimental methods, high reaction ability, friendly to environment, and high inhibition efficiency. We also investigated the inhibition efficiencies of AA-HPEZ to control $CaCO_3$ scale at higher temperatures and hardness environment, respectively.

2. Experimental setup

2.1. Materials

Sodium hydroxide, acrylic acid (AA), oxalic acid, hydrochloric acid, anhydrous calcium chloride, sodium bicarbonate, ethylenediaminetetraacetic acid disodium salt (EDTA·2Na), and ammonium persulfate of AR grade were obtained from Zhongdong Chemical Reagent (Nanjing, Jiangsu, China). Methallyl methoxy polyethylene glycol (HPEG; molecular weight = 300), poly(acrylic acid) (PAA; molecular weight = 1,800), poly(epoxysuccinic acid) (PESA; molecular weight = 1,500), and hydrolytic poly(maleic anhydride) (HPMA; molecular weight = 600) were obtained from Jianghai Reagent (Changzhou, Jiangsu, China). Distilled water was used for all the studies.

2.2. Synthesis of antiscalant

The synthesis procedure of HPEZ is shown in Fig. 1. It was synthesized from methallyl methoxy polyethylene glycol (HPEG) and oxalic acid at 80°C under nitrogen atmosphere for 4.0 h.

The synthesis procedure of AA-HPEZ is shown in Fig. 2. The copolymerization reaction was carried out in a 250 mL round-bottom flask with a mechanical stirrer, thermometer. About 0.15 mol (10.8 g) AA and 50 mL distilled water were mixed continuously with stirring under nitrogen atmosphere. Then, 0.05 mol (15 g) HPEZ and 50 mL distilled water were added in and heated to the reaction temperature of 65°C for about 0.5 h. In fixed conditions, the initiator ammonium persulfate was dropped at a certain flow rate for more than 1.0 h. Next, the reactant was heated with stirring at 80°C for 2.0 h under nitrogen atmosphere. At last, a faint yellow liquid with an approximately 28.0% solid content was obtained.

Antiscalant was synthesized at different mole ratio of AA:APEZ (3:1, 2:1, 1:1, 1:2, 1:3) to investigate the effect of mole ratio of AA:HPEZ on inhibition ability. The process was the same as initial feed mole ratio of AA:HPEZ was 3:1 in synthesis of antiscalant.

2.3. Measurements

The samples were analyzed by using an Fourier Transform infrared spectroscopy (FTIR) spectroscopy (VECTOR-22, Bruker Co., Germany) to confirm the functional groups in the pressed KBr pellets. Structures of HPEZ and AA-HPEZ were also explored by a Bruker NMR analyzer (AVANCE AV-500, Bruker, Switzerland) with a tetramethylsilane internal reference and deuterated dimethyl sulfoxide as the solvent. The shape of $CaCO_3$ and $CaSO_4$ scale was observed from a scanning electron microscopy (SEM; S-3400 N, Hitachi, Japan). Prior to imaging by SEM, the scale samples were sputtered with a thin layer of gold. The X-ray diffraction (XRD) studies

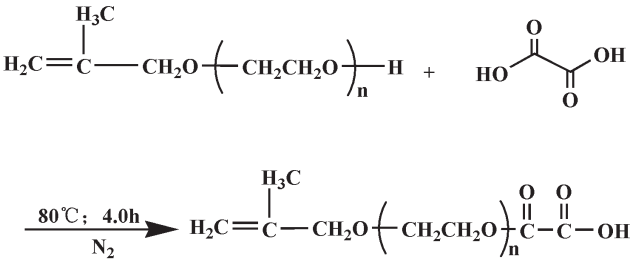

Fig. 1. Synthesis of HPEZ.

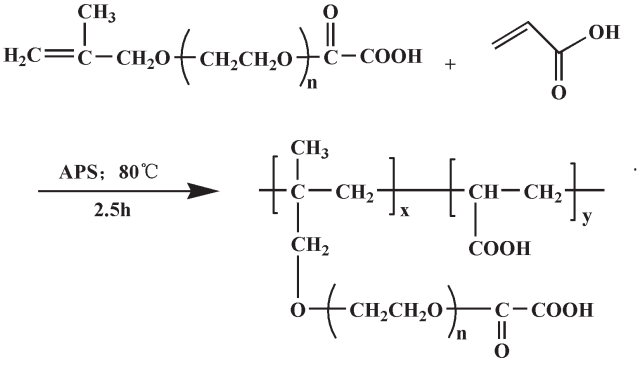

Fig. 2. Synthesis of AA-HPEZ.

were carry out by a Rigaku D/Max 2400 X-ray powder diffractometer with Cu Kα radiation (λ = 1.5406, 40 kV, 120 mA).

2.4. Static scale inhibition methods

The ability of the AA-HPEZ copolymer to inhibit $CaCO_3$ scale was compared with the blank test and all inhibitor dosages are given on a basis of dried conditions. The experiment was carried out in artificial cooling water, and the concentrations of Ca^{2+} and HCO_3^- were 240 and 732 mg/L, respectively. The artificial cooling water used in experiment was prepared by $NaHCO_3$ and $CaCl_2$ solution, with the solution pH 9 adjusting by borax buffer solution. According to the national standard of People's Republic of China (GB/T 16632–2008), every inhibition test was carried out in a 500 mL flask immersed at 80°C for 10.0 h in water bath. Then, it was cooled to room temperature. After that, the deposition of calcium carbonate was filtered out using filter paper, the filtrate was collected. At last, the concentration of Ca^{2+} ions in the supernatant was titrated by EDTA standard solution and compared with blank test according to standard methods (Water Treatment Reagent Unit of Standardization Research Institute of Chemical Industry of China Chemical Industry Press, 2003). At the end point of titration, the color of the solution changed from purple into blue by using calconcarboxylic acid indicator. Inhibitor efficiency was calculated from the following equation: [29]

$$\text{Inhibition efficiency (\%)} = \frac{(Ca^{2+})_1 - (Ca^{2+})_0}{(Ca^{2+})_2 - (Ca^{2+})_0} \times 100\% \quad (1)$$

where $(Ca^{2+})_0$ is the calcium ions concentration of uninhibited sample; $(Ca^{2+})_1$ is the calcium ions concentration of inhibited sample; and $(Ca^{2+})_2$ is the initial calcium ions concentration.

Procedure of calcium sulfate inhibition tests were carried alike to calcium carbonate precipitation experiments according to the national standard of People's Republic of China concerning the code for the design of industrial oilfield-water treatment (SY/T 5673-93). Calcium sulfate precipitation was studied in different artificial cooling water, and the concentrations of Ca^{2+} and SO_4^{2-} were 6,800 and 7,100 mg/L, respectively. The calcium sulfate solutions were prepared by dissolving a certain quantity of $CaCl_2$ and Na_2SO_4 in deionized water, and the pH of the solutions was adjusted to 7 using sodium hydroxide and hydrochloric acid. The artificial cooling water containing different doses of the AA-HPEZ was heated at 70°C for 6.0 h in a water bath. The determination of Ca^{2+} was done by the same process.

The entire test was taken for three times at the same experimental conditions. The scale inhibition data used in results part were the average data of the repeated tests.

3. Results and discussion

3.1. FTIR analysis of synthesized products

The FTIR spectra of HPEG (a), HPEZ (b), and AA-HPEZ (c) are exhibited in Fig. 3. Shallow and broad peak appeared around 3,450 cm^{-1} corresponds to –OH stretching vibrations of hydroxyl group. The emerging 1,742 cm^{-1} strong intensity absorption peak (–C=O) in curve (b) clearly reveals that

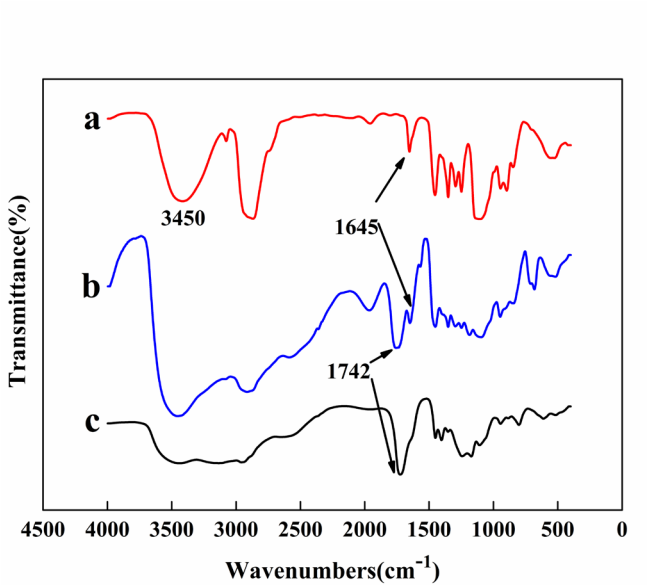

Fig. 3. FTIR spectra of: (a) HPEG, (b) HPEZ, and (c) AA-HPEZ.

HPEZ has been synthesized successfully [25]. The fact that the (–C=C–) stretching vibration at 1,645 cm^{-1} appears in curve (b) but disappears completely in curve (c) reveals that radical polymerization between AA and HPEZ has happened [14].

3.2. Hydrogen Nuclear magnetic resonance (^{1}H NMR) analysis of synthetic products

The ^{1}H NMR spectra of HPEG, HPEZ, and AA-HPEZ are presented in Fig. 4. HPEG (a) [$(CD_3)_2SO$, δ ppm]: 2.50 [solvent residual peak of $(CD_3)_2SO$], 3.30–3.60 (–OCH_2CH_2–, ether groups), 1.66 and 3.82–4.95 (CH_2=C (CH_3)–CH_2–, propenyl protons), and 4.50–4.60 (–OH, active hydrogen in HPEG).

HPEZ (b) [$(CD_3)_2SO$, δ ppm): 2.50 [solvent residual peak of $(CD_3)_2SO$], 3.40–4.32 (–OCH_2CH_2–, ether groups), and 1.66 and 4.33–4.95 (CH_2=C (CH_3)–CH_2–, methyl allyl protons).

AA-HPEZ (c) [$(CD_3)_2SO$, δ ppm]: 2.50 [solvent residual peak of $(CD_3)_2SO$], 1.45–1.78 (–CH_3, methyl proton), and 3.30–3.90 (–OCH_2CH_2–, ether groups).

The complete disappearance of 4.50–4.60 ppm (–OH) active hydrogen in (a) proves that active hydroxyl group in HPEG has reacted with oxalic acid [24]. Furthermore, 4.80–4.95 ppm in (b) double bond absorption peaks completely disappeared in (c). This result reveals that free radical polymerization among AA and HPEZ has happened. From FTIR and ^{1}H NMR analysis, it can conclude that synthesized AA-HPEZ has anticipated structure.

3.3. Carbon thirteen Nuclear magnetic resonance (^{13}C NMR) analysis of synthetic products

The method of ^{13}C NMR was used to analyze the structure of oxalic acid, HPEG and HPEZ with deuterated dimethyl sulfoxide as the solvent, as shown in Fig. 5. As can be seen from Fig. 5, the peak appeared around 44.34 ppm can be attributed to the solvent residual peak of $(CD_3)_2SO$. The unique peak at 166.03 ppm in curve (a) is assigned to

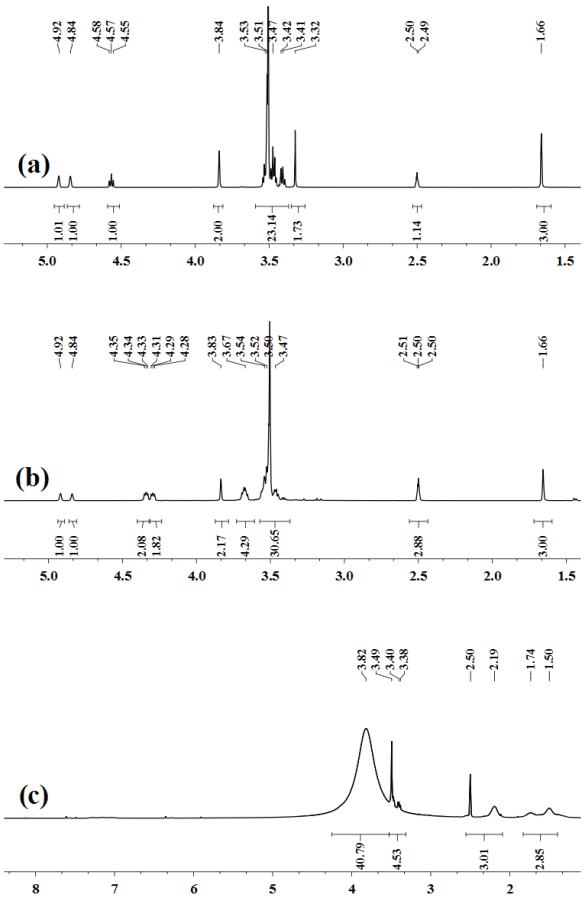

Fig. 4. ^{1}H NMR spectra of: (a) HPEG, (b) HPEZ, and (c) AA-HPEZ.

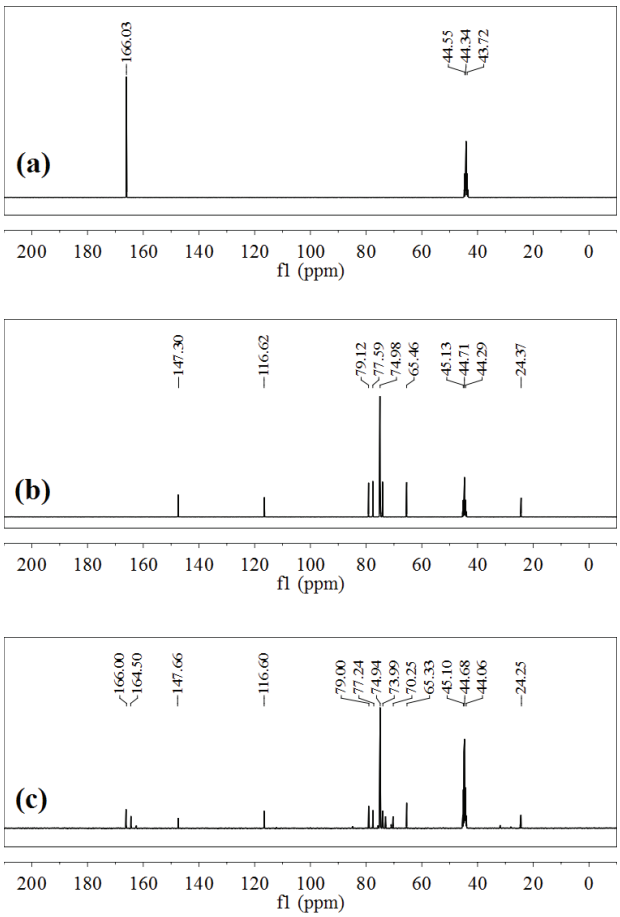

Fig. 5. ^{13}C NMR spectra of: (a) oxalic acid, (b) HPEG, and (c) HPEZ.

the carbonyl carbons of oxalic acid. The peaks from 65 to 80 ppm are attributed to the ether groups (–CH_2CH_2O–) in Figs. 5(b) and (c). However, compared with curve (b), there are two peaks appeared at 164.50 and 166.00 ppm in curve (c), which the former is assigned to the ester group near ethyl group and the latter is assigned to the terminal carboxyl group of HPEZ. The oxy-ethyl group is an electron donating group, which will reduce the chemical shift value of the carbonyl carbons. These results indicate that the hydroxyl group in HPEZ has reacted with oxalic acid.

3.4. Effect of inhibitor on $CaCO_3$ and $CaSO_4$

Concentration and mole ratio of AA and HPEZ greatly influence the performance of antiscalant. The scale inhibition performance of AA-HPEZ at different mole ratio of AA:HPEZ in simulated scale inhibition solution toward $CaCO_3$ and $CaSO_4$ are shown in Tables 1 and 2, respectively.

Table 1 indicates that under the same experimental conditions, the dosage of AA-HPEZ and the mole ratio of AA with HPEZ have a strong effect on the formation of calcium carbonate precipitation. As can be seen, the scale inhibition efficiency strengthened with the increasing concentration of the inhibitors. The inhibition efficiency obtained from AA-HPEZ (AA:HPEZ = 2:1) at a concentration of 8 mg/L is about 90.6%, and it is about 79.8%, 67.8%, 59.8%, and 57.5% at different mole ratio (3:1, 1:1, 1:2, and 1:3) at the same concentration.

Table 1
Influences of the dosage and mole ratio on the inhibition tests to $CaCO_3$

Dosage of inhibitor (mg/L)	Inhibition efficiency (%)				
	3:1	2:1	1:1	1:2	1:3
2	37.1	47.9	40.2	32.1	36.2
4	50.3	65.1	48.4	47.4	42.3
6	62.4	73.2	59.3	52.3	45.1
8	79.8	90.6	67.8	59.8	57.5
10	79.4	90.0	72.0	64.0	61.7
12	79.1	89.2	73.7	70.5	64.9
14	80.0	90.5	72.2	71.9	65.4
16	80.1	88.8	73.9	72.2	65.8
18	82.2	89.4	73.8	71.7	64.7

Influence of the dosage and mole ratio of AA-HPEZ on the inhibition tests to calcium sulfate can be seen from Table 2. The inhibition value is 100% at a level of 4 mg/L (AA:HPEZ = 2:1), while it is 85.8%, 88.4%, 89.8%, and 82.5%

Table 2
Influences of the dosage and mole ratio on the inhibition tests to $CaSO_4$

Dosage of inhibitor (mg/L)	Inhibition efficiency (%)				
	3:1	2:1	1:1	1:2	1:3
1	67.6	77.3	60.3	59.3	53.1
2	72.1	87.2	69.1	70.4	69.3
3	78.6	92.8	78.4	76.1	77.6
4	85.8	100	88.4	89.8	82.5
5	91.9	99.4	90.7	93.5	87.4
6	93.5	100	94.5	92.9	90.3
7	93.4	99.7	95.2	93.4	91.1
8	95.1	100	95.1	93.5	91.4
9	94.6	100	94.9	93.9	90.9

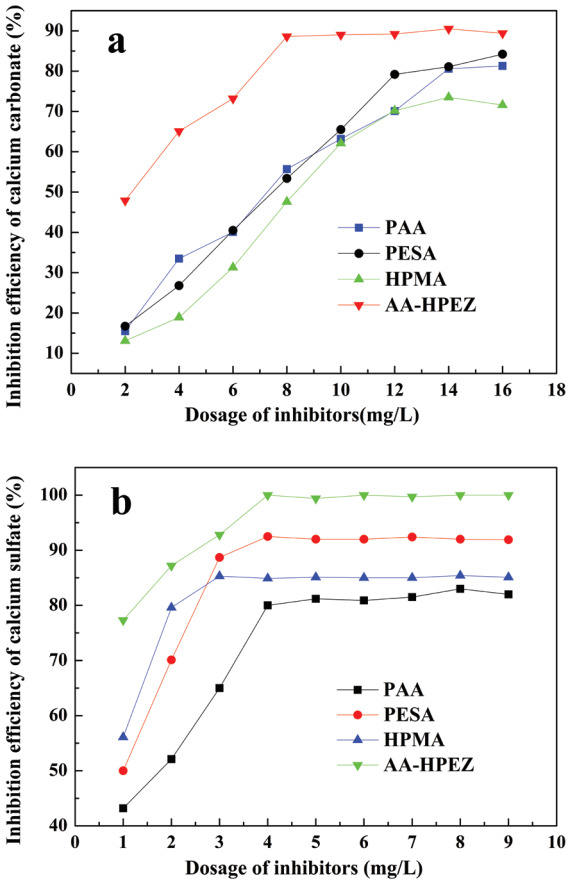

Fig. 6. Comparison of scale inhibition efficiency on $CaCO_3$ (a) and $CaSO_4$ (b) between AA-HPEZ and different commercial inhibitor.

at the same dosage with different mole ratio of AA with HPEZ (3:1, 1:1, 1:2, and 1:3), respectively.

The mole ratio (AA:HPEZ = 2:1) compared with the other mole ratio exhibits superior performance to inhibit $CaCO_3$ and $CaSO_4$ scale. As a result, the best mole ratio of AA-HPEZ is 2:1 which can ensure the maximum effect for both $CaCO_3$ and $CaSO_4$. The inhibition efficiency reached 90.6% and 100% for $CaCO_3$ and $CaSO_4$ at dose of 8 and 4 mg/L, respectively.

3.5. Comparisons of inhibition efficiency

To understand the performance of AA-HPEZ, the ability of AA-HPEZ (AA:HPEZ = 2:1) to control calcium deposits was compared with PAA, PESA, and HPMA at identical conditions.

It can be seen from Fig. 6(a) that the order of the inhibition efficiency of $CaCO_3$ is AA-HPEZ > PAA ≈ PESA > HPMA. Compared with commercial inhibitors, AA-HPEZ shows superior ability in inhibiting $CaCO_3$ scale, and anti-scaling rate reached the highest which is 90.6% at the threshold dosage of 8 mg/L, whereas it is 55.7% for PAA at the same dosage (the best inhibitor among them). As shown in Fig. 6(b), it indicates that the order of preventing the precipitation of $CaSO_4$ is AA-HPEZ > PESA > HPMA > PAA, the ultimate inhibition efficiency values are 100%, 91.3%, 86.6%, and 81.2% at the threshold dosage of 4 mg/L, respectively. The data in Fig. 6 indicate that AA-HPEZ can be used as an efficient scale inhibitor for $CaCO_3$ and $CaSO_4$ in cooling water systems. On the basis of the test results, AA-HPEZ (2:1) is chosen in the following tests.

3.6. Effect of Ca^{2+} concentration on inhibition efficiency to $CaCO_3$ scale

The inhibition efficiency of AA-HPEZ is investigated under conditions of water with higher hardness. Fig. 7 represents the effect of Ca^{2+} concentration on the scale inhibition efficiency of AA-HPEZ against $CaCO_3$. With other conditions remaining unchanged, the scale inhibition efficiency of copolymers decreased with increasing Ca^{2+}. Even Ca^{2+} reaches a certain value the $CaCO_3$ scale could also be significantly inhibited at relatively low inhibitor concentrations. The results indicate that AA-HPEZ is an effective inhibitor which can be used in a water system with higher hardness.

3.7. Effect of temperature on inhibition efficiency to $CaCO_3$ scale

The effects of temperature on the scale inhibition efficiency for scaling $CaCO_3$ are shown in Fig. 8. As can be seen from Fig. 8, AA-HPEZ copolymer shows superior $CaCO_3$ inhibition efficiency at the usual temperature values of industry cooling water systems (60°C–80°C). When the solution temperature increased to 90°C, the inhibition efficiency still exceeded 80.0% at the dosage of 8 mg/L. We infer that AA-HPEZ copolymer possesses the advantage of good thermal tolerance because of the side chain with functional groups. Therefore, AA-HPEZ can also be used as an effective inhibitor in cooling water systems at high temperature.

3.8. Morphology characterization of calcium scale

3.8.1. SEM analysis of $CaCO_3$ and $CaSO_4$ crystals

In order to better analyze the influence of scale inhibitor on the growth and morphology of $CaCO_3$ and $CaSO_4$ crystal, AA-HPEZ was used as an inhibitor in the experiment, and

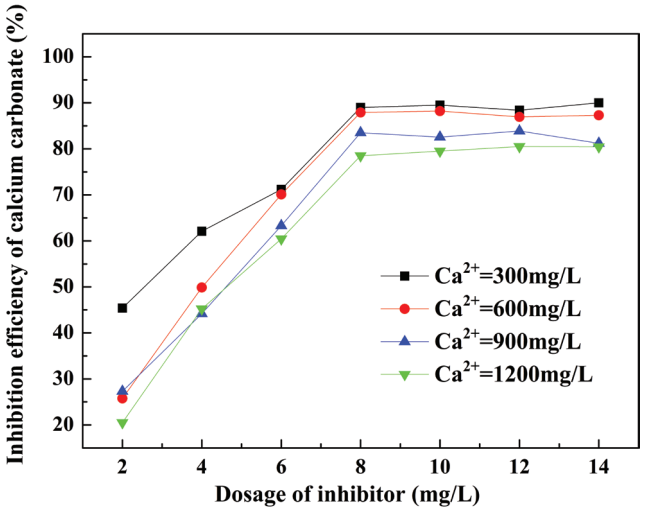

Fig. 7. Effect of Ca^{2+} concentrations on inhibition efficiency to $CaCO_3$ scale.

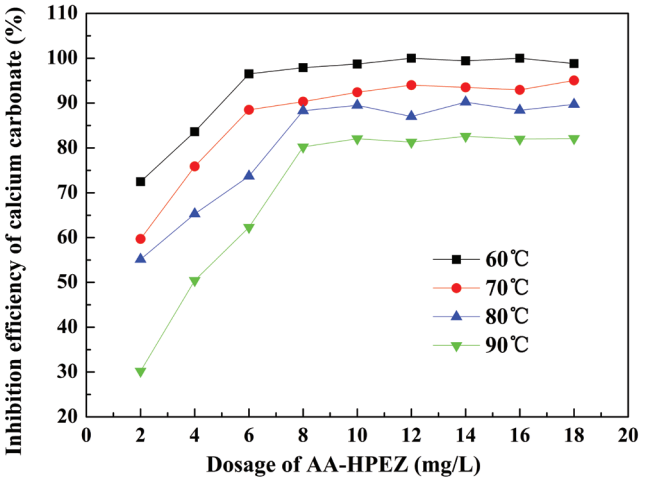

Fig. 8. Effect of temperature on the inhibition efficiency to $CaCO_3$ scale.

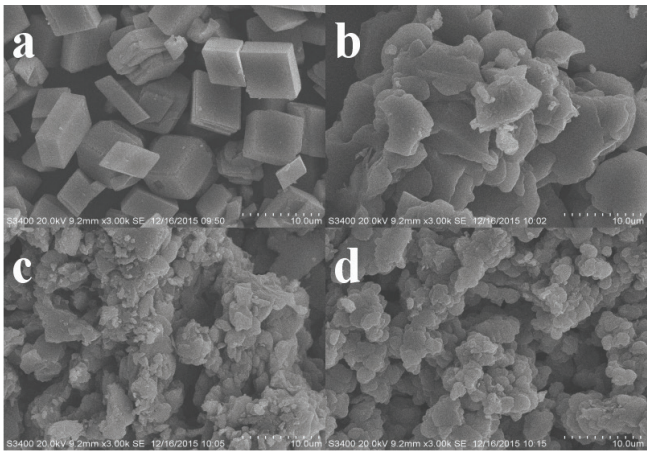

Fig. 9. SEM photographs for the calcium carbonate: (a) without the presence of AA-HPEZ, (b) 2 mg/L, (c) 4 mg/L, and (d) 6 mg/L.

the collected $CaCO_3$ and $CaSO_4$ scales were characterized by SEM analyses.

Fig. 9 exhibited the influence of the AA-HPEZ copolymer on the morphologies of $CaCO_3$. The $CaCO_3$ deposits that formed in the absence of AA-HPEZ are symmetrical and block like particles of cubic shape or rhombohedral (Fig. 9(a)). In contrast, the well-regulated structure is damaged and it has obvious changes at the distribution and size on addition of 2 mg/L of the additive (Fig. 9(b)). Flower- and cascade-like agglomerated $CaCO_3$ deposits are obtained with the increasing dosage of AA-HPEZ (Figs. 9(c) and (d)). AA-HPEZ contains functional groups like carboxyl which could effectively adsorb at the surface of calcite and break the structure of calcite [30]. In this case, the scales are hardly attached to the pipe surface and could be easily removed with enough shear force from flowing water.

The SEM photographs of $CaSO_4$ scale with and without the presence of the AA-HPEZ are presented in Fig. 10. The crystals of $CaSO_4$ are regular rod-shaped and look like thin tubular cells exhibiting monoclinic symmetry (Fig. 10(a)) [6]. However, with the addition of AA-HPEZ, the sharp edges and acute corners of the $CaSO_4$ crystals changed completely into loose structure and defective rod (Fig. 10(b)). Therefore, the soft scale could be easily washed away by water because morphology of $CaSO_4$ was changed.

3.8.2. XRD analysis of $CaCO_3$ and $CaSO_4$ crystals

The XRD methods were used to monitor the structural changes of the $CaCO_3$ precipitation (Fig. 11). It is generally known that $CaCO_3$ have three types of crystal forms: calcite, aragonite, and vaterite [22]. Fig. 11(a) demonstrates that the diffraction peaks of the precipitates of $CaCO_3$ could be well indexed to the calcite phase, which is the most thermodynamically stable crystal. This result indicates that the crystal of calcium carbonate is mainly an ingredient of calcite without addition of AA-HPEZ. However, the intensity of calcite phase peaks is lower than that of blank samples, and both the intense peaks of calcite and vaterite have been observed in Fig. 11(b). Thus, synthesized inhibitors could inhibit or disturb the calcite growth and induce vaterite growth.

The XRD results for sulfate calcium crystals in the absence of AA-HPEZ and in the presence of AA-HPEZ are presented in Fig. 12. The interplanar crystal spacing and angle of intersection values conformed to the structure of gypsum ($CaSO_4{\cdot}2H_2O$, calcium sulfate dehydrate, Fig. 12(a)) [31]. However, Fig. 12(b) shows that there is no modification in the crystal structure. Modification of the morphology can only be observed from the SEM photographs (Fig. 10(b)).

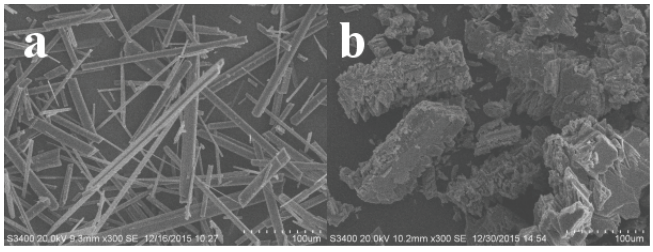

Fig. 10. SEM photographs for the calcium sulfate: (a) without the presence of AA-HPEZ and (b) 2 mg/L.

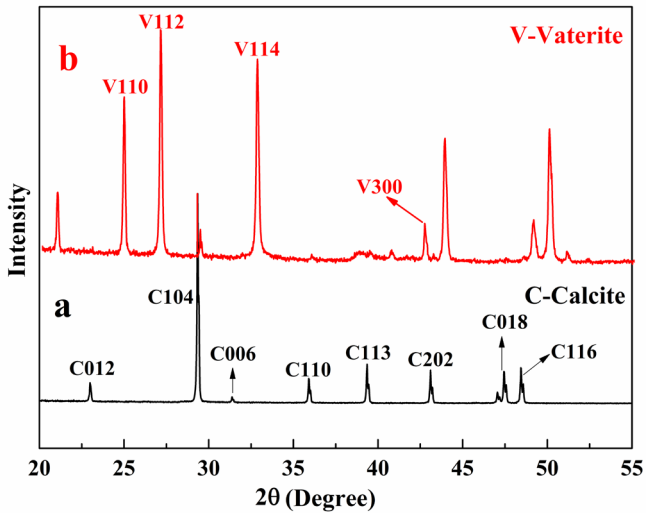

Fig. 11. XRD images of the $CaCO_3$ crystal formed (a) in the absence of AA-HPEZ and (b) with the presence of AA-HPEZ.

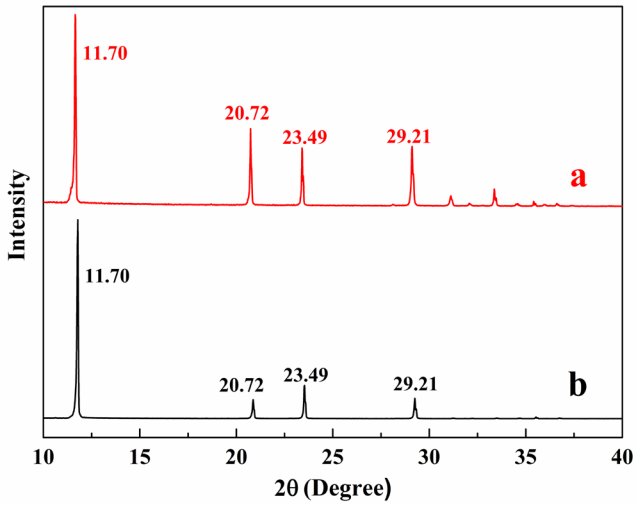

Fig. 12. XRD images of the $CaSO_4$ crystal formed (a) in the absence of AA-HPEZ and (b) with the presence of AA-HPEZ.

3.8.3. FTIR analysis of $CaCO_3$ crystals

FTIR is another characterization technique used to identify the various polymorphs present in the crystals. The FTIR spectra of the calcium carbonate precipitates obtained in the absence and presence of the AA-HPEZ are shown in Fig. 13. As shown by the curve (a), the peaks given at 874 and 712 cm^{-1} could be attributed to the vibrations of calcite [32]. On the other hand, a new peak (745 cm^{-1}) is observed in curve (b), which reflects the vibrations in the vaterite form. In addition, there is no intensity of the band at 712 cm^{-1} in curve (b), which means the portion of vaterite increased. The addition of AA-HPEZ has a great influence on the FTIR observation. All the data of the FTIR spectra demonstrate that the new scale inhibitor can affect the polymorphs of the calcium carbonate crystals.

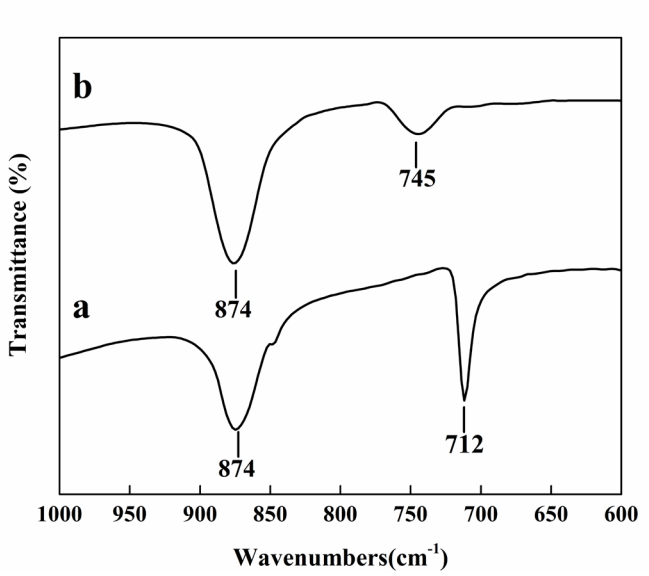

Fig. 13. FTIR spectra of calcium carbonate precipitates formed (a) in the absence of the AA-HPEZ and (b) in the presence of 6 mg/L AA-HPEZ.

3.9. The mechanism of calcium scale inhibition

The above results indicate that with the presence of AA-HPEZ, the structure of calcium scales and crystal morphology are modified. Kinds of theories about the mechanism of calcium scales inhibition were reported, such as chelating solubilization and electrostatic repulsion function [33].

AA-HPEZ is a structurally well-defined bi-block copolymer consisting of a polyethylene glycol (PEG) matrix and a large number of carboxyl groups (–COOH) which can easily ionize to $–COO^-$. Both the –COOH groups and the PEG matrix play an important role in inhibiting the scale precipitation. The carboxyl groups in AA-HPEZ can encapsulate or capture Ca^{2+} either in solutions or on the surface of inorganic minerals [29,34]. Moreover, Ca^{2+} also interact with these negatively charged ions (SO_4^{2-} and CO_3^{2-}) and form $CaCO_3$ and $CaSO_4$ crystal embryos. As a consequence, these calcium ions serving as bridges link AA-HPEZ by carboxyl groups and SO_4^{2-} or CO_3^{2-} ions by an electrostatic attractive force. Simultaneously, the surfaces of $CaCO_3$ and $CaSO_4$ crystal embryos are surrounded by long side chains of AA-HPEZ (PEG segments), and toward stable aqueous phase because of the strong hydrogen bonding between water molecules and carboxyl groups. As a result, the aggregation of $CaCO_3$ and $CaSO_4$ solid particles is blocked. In addition, the long PEG side chains in AA-HPEZ matrix result in steric and electrostatic repulsion. Therefore, the existing minerals do not precipitate in the presence of AA-HPEZ owing to its excellent ability to disperse solid particles.

4. Conclusion

A novel effective antiscalant (AA-HPEZ) was successfully synthesized by free copolymerization, and the structure was characterized by FTIR and ^1H NMR. The inhibition

efficiencies of AA-HPEZ toward $CaCO_3$ and $CaSO_4$ scales were 90.6% and 100% at the dosage of 8 and 4 mg/L, respectively. Compared with the commercial inhibitors of PAA, PESA, and HPMA; AA-HPEZ shows an excellent inhibitory efficiency both on calcium sulfate and calcium carbonate precipitation. Meanwhile, the inhibition efficiency of AA-HPEZ against $CaCO_3$ scales still exceeded 80.0% when the temperature increased to 90°C. With the Ca^{2+} concentration increased to 1,200 mg/L the inhibition efficiency to $CaCO_3$ scales obtained still exceeded 80.0%. These results indicate that AA-HPEZ had good chemical stability at elevated temperatures and can be used in a water system with higher hardness. From the studies of SEM, XRD, and FTIR on the deposition of calcium carbonate and calcium sulfate, the copolymer had a great impact on the growth rate and the morphology of calcium crystals. These results indicate that AA-HPEZ can be used as an effective and environmentally friendly scale inhibitor for circulating cooling water systems.

Acknowledgments

This work was supported by the Prospective Joint Research Project of Jiangsu Province (BY2016076-01); the National Natural Science Foundation of China (51673040); Scientific Innovation Research Foundation of College Graduate in Jiangsu Province (KYLX16_0266); a Project Funded by the Priority Academic Program Development of Jiangsu Higher Education Institutions (PAPD1107047002); The Fundamental Research Funds for the Central Universities (3207046302); Fund Project for Transformation of Scientific and Technological Achievements of Jiangsu Province of China (BA2016105); and Based on Teachers' scientific research SRTP of southeast University (T16192003).

References

[1] M.M. Vazirian, T.V.J. Charpentier, M.D.O. Penna, A. Neville, Surface inorganic scale formation in oil and gas industry: as adhesion and deposition processes, J. Pet. Sci. Eng., 137 (2016) 22–32.
[2] D.E. Abd-El-Khalek, B.A. Abd-El-Nabey, M.A. Abdel-kawi, S.R. Ramadan, Investigation of a novel environmentally friendly inhibitor for calcium carbonate scaling in cooling water, Desal. Wat. Treat., 57 (2016) 2870–2876.
[3] H. Li, M.K. Hsieh, S.H. Chien, J.D. Monnell, D.A. Dzombak, R.D. Vidic, Control of mineral scale deposition in cooling systems using secondary-treated municipal wastewater, Water Res., 45 (2011) 748–760.
[4] N. Dhakal, S.G.S. Rodriguez, J.C. Schippers, M.D. Kennedy, Induction time measurements in two brackish water reverse osmosis plants for calcium carbonate precipitation, Desal. Wat. Treat., 53 (2014) 285–293.
[5] H.X. Zhang, Z.Y. Cai, X.H. Jin, D.X. Sun, D.D. Wang, T.R. Yang, J. Zhang, X. Han, Preparation of modified oligochitosan and evaluation of its scale inhibition and fluorescence properties, J. Appl. Polym. Sci., 132 (2015) 42518–42528.
[6] F.A. Setta, A. Neville, Efficiency assessment of inhibitors on $CaCO_3$ precipitation kinetics in the bulk and deposition on a stainless steel surface (316L), Desalination, 281 (2011) 340–347.
[7] A.L. Kavitha, T. Vasudevan, H.G. Prabu, Evaluation of synthesized antiscalants for cooling water system application, Desalination, 268 (2011) 38–45.
[8] R. Ketrane, B. Saidani, O. Gil, L. Leleyter, F. Baraud, Efficiency of five scale inhibitors on calcium carbonate precipitation from hard water: effect of temperature and concentration, Desalination, 249 (2009) 1397–1404.
[9] X. Li, B. Gao, Q. Yue, D. Ma, H. Rong, P. Zhao, P. Teng, Effect of six kinds of scale inhibitors on calcium carbonate precipitation in high salinity wastewater at high temperatures, J. Environ. Sci., 29 (2015) 124–130.
[10] Z. Shen, J. Li, K. Xu, L. Ding, H. Ren, The effect of synthesized hydrolyzed polymaleic anhydride (HPMA) on the crystal of calcium carbonate, Desalination, 284 (2012) 238–244.
[11] M. Gloede, T. Melin, Physical aspects of membrane scaling, Desalination, 224 (2008) 71–75.
[12] A.A. Al-Hamzah, C.M. Fellows, A comparative study of novel scale inhibitors with commercial scale inhibitors used in seawater desalination, Desalination, 359 (2015) 22–25.
[13] K.D. Demadis, S.D. Katarachia, M. Koutmos, Crystal growth and characterization of zinc–(amino-*tris*-(methylenephosphonate)) organic–inorganic hybrid networks and their inhibiting effect on metallic corrosion, Inorg. Chem. Commun., 8 (2005) 254–258.
[14] H.C. Wang, Y.M. Zhou, Q.Z. Yao, W. Sun, Calcium sulfate precipitation studies with fluorescent-tagged scale inhibitor for cooling water systems, Polym. Bull., 72 (2015) 2171–2188.
[15] P. Shakkthivel, T. Vasudevan, Newly developed itaconic acid copolymers for gypsum and calcium carbonate scale control, J. Appl. Polym. Sci., 103 (2007) 3206–3213.
[16] Y. Liu, C. Zou, C. Li, L. Lin, W. Chen, Evaluation of β-cyclodextrin–polyethylene glycol as green scale inhibitors for produced-water in shale gas well, Desalination, 377 (2016) 28–33.
[17] H.K. Can, U. Gizem, Water-soluble anhydride containing alternating copolymers as scale inhibitors, Desalination, 355 (2015) 225–232.
[18] D.J. Choi, S.J. You, J.G. Kim, Development of an environmentally safe corrosion, scale, and microorganism inhibitor for open recirculating cooling systems, Mater. Sci. Eng., A, 335 (2002) 228–235.
[19] M.M. Reddy, A.R. Hoch, Calcite crystal growth rate inhibition by polycarboxylic acids, J. Colloid Interface Sci., 235 (2001) 365–370.
[20] Y.M. Al-Roomi, K.F. Hussain, Application and evaluation of novel acrylic based $CaSO_4$ inhibitors for pipes, Desalination, 355 (2015) 33–44.
[21] J. Feng, L. Gao, R. Wen, Y. Deng, X. Wu, S. Deng, Fluorescent polyaspartic acid with an enhanced inhibition performance against calcium phosphate, Desalination, 345 (2014) 72–76.
[22] X.Y. Sun, J.P. Zhang, C.X. Yin, J.T. Zhang, J. Han, Poly(aspartic acid)–tryptophan grafted copolymer and its scale-inhibition performance, J. Appl. Polym. Sci., 132 (2015) 42739–42747.
[23] Y. Li, C. Yang, Y. Zhang, J. Zheng, H. Guo, M. Lu, Study on dispersion, adsorption and flow retaining behaviors of cement mortars with TPEG-type polyether kind polycarboxylate superplasticizers, Constr. Build. Mater., 64 (2014) 324–332.
[24] H. Wang, Y. Zhou, Q. Yao, S. Ma, W. Wu, W. Sun, Synthesis of fluorescent-tagged scale inhibitor and evaluation of its calcium carbonate precipitation performance, Desalination, 340 (2014) 1–10.
[25] Y. Liu, Y. Zhou, Q. Yao, W. Sun, Evaluating the performance of PEG-based scale inhibition and dispersion agent in cooling water systems, Desal. Wat. Treat., 56 (2014) 1309–1320.
[26] Y. Chen, Y. Zhou, Q. Yao, Y. Bu, H. Wang, W. Wu, W. Sun, Evaluation of a low-phosphorus terpolymer as calcium scales inhibitor in cooling water, Desal. Wat. Treat., 55 (2014) 945–955.
[27] Y. Bu, Y. Zhou, Q. Yao, Y. Chen, W. Sun, W. Wu, Inhibition of calcium carbonate and sulfate scales by a non-phosphorus terpolymer AA-APEY-AMPS, Desal. Wat. Treat., 57 (2014) 1977–1987.
[28] H. Wang, Y. Zhou, G. Liu, J. Huang, Q. Yao, S. Ma, K. Cao, Y. Liu, W. Wu, W. Sun, Z. Hu, Investigation of calcium carbonate precipitation in the presence of fluorescent-tagged scale inhibitor for cooling water systems, Desal. Wat. Treat., 53 (2013) 3491–3498.
[29] NACE Standard Test Method, Laboratory Screening Test to Determine the Ability to Scale Inhibitors to Prevent the Precipitation of Calcium Sulfate and Calcium Carbonate from Solution, TM 0374-2001, Item 21208, 2001.

[30] D.J. Tobler, J.D. Rodriguez-Blanco, K. Dideriksen, N. Bovet, K.K. Sand, S.L.S. Stipp, Citrate effects on amorphous calcium carbonate (ACC) structure, stability, and crystallization, Adv. Funct. Mater., 25 (2015) 3081–3090.
[31] X. Mao, X. Song, G. Lu, Y. Xu, Y. Sun, J. Yu, Effect of additives on the morphology of calcium sulfate hemihydrate: experimental and molecular dynamics simulation studies, Chem. Eng. J., 278 (2015) 320–327.
[32] S.H. Yu, H. Colfen, M. Antonietti, Polymer-controlled morphosynthesis and mineralization of metal carbonate superstructures, J. Phys. Chem. B, 107 (2003) 7396–7405.
[33] G. Liu, J. Huang, Y. Zhou, Q. Yao, H. Wang, L. Ling, P. Zhang, K. Cao, Y. Liu, W. Wu, W. Sun, Carboxylate-terminated double-hydrophilic block copolymer containing fluorescent groups: an effective and environmentally friendly inhibitor for calcium carbonate scales, Int. J. Polym. Mater. Polym. Biomater., 62 (2013) 678–685.
[34] S. Lee, C.H. Lee, Effect of operating conditions on $CaSO_4$ scale formation mechanism in nanofiltration for water softening, Water Res., 34 (2000) 3854–3866.